The Journal of Immunology

# Triggering of T Cell Activation via CD4 Dimers



Maria-Cristina Moldovan, Laurent Sabbagh, Gaëlle Breton, Rafick-Pierre Sékaly and Matthew F. Krummel

*J. Immunol.* 2006;176;5438-5445
http://www.jimmunol.org/cgi/content/full/176/9/5438



*The Journal of Immunology* is published twice each month by The American Association of Immunologists, Inc., 9650 Rockville Pike, Bethesda, MD 20814-3994.

Print ISSN: 0022-1767 Online ISSN: 1550-6606.

# Triggering of T Cell Activation via CD4 Dimers[1]

**Maria-Cristina Moldovan,*† Laurent Sabbagh,* Gaëlle Breton,‡ Rafick-Pierre Sékaly,[2,3]*‡ and Matthew F. Krummel[2†]**

**The onset of activation in Th cells is triggered by localized coengagement of TCRs and the coreceptor CD4. A CD4 crystal suggested that CD4 may form dimers in some circumstances. In this study, we use live-cell fluorescence resonance energy transfer imaging to demonstrate that CD4 dimers are present at a basal level on the cell surface and accumulate at the synapse. Mechanistically, we reveal two conditions under which dimers are highly relevant. First, CD4 dimers are more proficient in mediating prolonged cell contacts with APCs in the presence or absence of Ag. This is consistent with a model whereby the dimer functions to increase T-APC avidity. Second, we show that dimer mutations result in an increased level of an inactive lckTyr$^{505}$ bound to the CD4 molecule relative to dimer-competent CD4. We also find a consistent defect in signaling onset in these cells. This supports a role for CD4 dimerization in maintaining active signaling machinery. We suggest that modulation of the dimer/monomer ratio may permit tuning of activation thresholds during initial engagement.** *The Journal of Immunology,* **2006, 176: 5438–5445.**

The adaptive immune response is activated when TCRs on the surface of CD4$^+$ T lymphocytes recognize peptides that are bound to MHC class II molecules on the surface of APCs. The CD4 coreceptor binds to a peptide-independent region of MHC and increases T cell sensitivity to Ag by 10- to 100-fold (1–4). This role is most prominent at suboptimal stimulation conditions, that is either low ligand concentration or poor affinity of the TCR for the MHC-peptide complex (3–6).

There are two proposed mechanisms by which CD4 may trigger T cell activation. First, in binding the TCR-pMHC complex, CD4 recruits the associated p56$^{lck}$ kinase, thus potentiating Ag-dependent signal transduction (7–10). Second, CD4 binding to MHC class II may enhance cell-cell adhesion, tethering MHC molecules and thereby increasing TCR occupancy (11–14). However, in solution, monomeric CD4 possesses poor pMHC binding ($K_d$ = 200 $\mu$M) with no detectable affinity for the TCR (15), thus raising questions of how it contributes to TCR triggering in this way.

The crystal structure of the entire extracellular (D1-D4) portion of CD4 showed weak homodimerization (estimated $K_d$ of 44.3 mg ml$^{-1}$) (16). This raised the possibility that the weak monomeric CD4-MHC affinity could be overcome by augmenting the avidity of the interaction through CD4 dimerization/oligomerization. Several crystallographic, molecular modeling, biochemical, and functional studies have indicated the involvement of CD4 oligomers in MHC class II binding and/or T cell activation (12, 17–22). Confirming the crystallographic data, we identified K318 and Q344, two highly conserved residues within the D4 domain, as critical for CD4 dimer formation, assessed biochemically. Although we have shown that CD4 dimers constitute the functional component of CD4 for cytokine production, the mechanism involved is unclear (23).

Recent studies have established that T cell activation is characterized by the formation of an immunological synapse (IS)[4] between the T cells and their cognate APCs (24, 25). On Th lymphocytes, the CD4 coreceptor is a critical player in the early stages of synapse formation, serving to boost recognition of pMHC by the TCR (4, 26) and to facilitate efficient p56$^{lck}$ recruitment in the vicinity of the engaged TCR-CD3 complex (10). Interestingly, once activation has been triggered and a mature IS is formed, a bulk of CD4 is excluded from the central synapse, suggesting that it may no longer be required (26, 27).

Recent technological progress has improved our ability to visualize the T cell-APC interface. For example, three-dimensional video microscopy of proteins labeled with fluorescent tags has provided great insight into the molecular dynamics and requirements involved in the formation of the IS. In addition, fluorescence resonance energy transfer (FRET) measurements using two matched fluorophores in close proximity can be used to monitor protein-protein interactions (28–30).

In this study, we have generated fluorescently tagged CD4 molecules to examine the temporal dynamics and kinetic requirements for dimers during recognition of superantigen staphylococcal enterotoxin B (SEB). Using live cell imaging of FRET between CD4 molecules, either wild type (wt) or deficient in their ability to dimerize, we show that dimerization potentiates couple formation, signaling commitment, and CD4 accumulation in the contact area, but monomeric CD4-bearing cells are capable of supporting prolonged responses, once initiation has occurred. Furthermore, real-time FRET analysis provides evidence of an even closer apposition

*Department of Microbiology and Immunology, McGill University, Montréal, Canada; †Department of Pathology, University of California, San Francisco, CA 94143; and ‡Département de Microbiologie et Immunologie, Université de Montréal, Montréal, Canada

Received for publication July 25, 2005. Accepted for publication February 15, 2006.

The costs of publication of this article were defrayed in part by the payment of page charges. This article must therefore be hereby marked *advertisement* in accordance with 18 U.S.C. Section 1734 solely to indicate this fact.

[1] L.S. was supported by the Fonds de la Recherche en Santé du Québec Fond de Recherche en Santé du Quebec-Fonds pour la Formation de Chercheurs et l'Aide a la Recerche-Santé doctoral research bursary, and was a recipient of the Doctoral Research Award from the Canadian Institutes for Health Research. R.-P.S. was funded by Canadian Institute of Health Research and the Canada Research Chair in Human Immunology. M.F.K. was funded by start up funds from the Howard Hughes Medical Institute Biomedical Research Support Program Grant 5300246.

[2] R.-P.S. and M.F.K. contributed equally to this work.

[3] Address correspondence and reprint requests to Dr. Rafick-Pierre Sékaly, Laboratoire d' Immunologie, Département de Microbiologie et Immunologie, Université de Montréal, CP. 6128, Succursale Centre ville, Montréal (Québec) H3C 3J7, Canada. E-mail address: rafick-pierre.sekaly@umontreal.ca

[4] Abbreviations used in this paper: IS, immunological synapse; CD4mut, CD4 mutant; CFP, cyan fluorescent protein; DIC, differential interference contrast; E, energy transfer efficiency; FRET, fluorescence resonance energy transfer; SEB, staphylococcal enterotoxin B; wt, wild type; YFP, yellow fluorescent protein.



0022-1767/06/$02.00

of CD4 molecules, indicating the formation of higher order complexes at later stages.

## Materials and Methods

### *Constructs and generation of cell transfectants*

CD4 fusion constructs were generated by attaching enhanced YFP or CFP (BD Clontech) to the C termini of CD4wt or CD4K318E. cDNAs encoding these constructs were subcloned into the retroviral vector pIB-2 (27). The 3DT52.5.8 is a murine CD4-negative T cell hybridoma subclone (31, 32). We generated clonal populations of 3DT52.5.8 cells stably expressing similar surface levels of CD4wt-cyan fluorescent protein (CFP) and CD4wt-yellow fluorescent protein (YFP) molecules, or CD4K318E-CFP and CD4K318E-YFP molecules as described (33). The murine B cell lymphoma cell line A20 (34) or DAP-DR1 fibroblasts (17) were used as APCs.

### *Antibodies*

L-68 and OKT4 are mouse mAbs specific to human CD4 (17, 35). The rat anti-mouse CD3 Ab 145-2C11 was produced in our laboratory (36). The 4G10 anti-phosphotyrosine mAb was purchased from Upstate Biotechnology, phospho-lck ($Tyr^{505}$) Ab from Cell Signaling Technology, and anti-phosphotyrosine-PE Ab (PY20) from BD Pharmingen.

### *Stimulation assays and measurement of IL-2 production*

A total of $7.5 \times 10^4$ T cells was cocultured with $2.5 \times 10^4$ A20 cells in the presence of increasing doses (0.5, 1, 5, and 10 mg $ml^{-1}$) of superantigen SEB (Toxin Technology) for 20 h at 37°C. For anti-CD3 stimulation, $7.5 \times 10^4$ T cells were cultured in anti-CD3-coated wells (0, 0.01, 0.1, and 1 mg $ml^{-1}$) for 20 h at 37°C. The supernatants were harvested, and levels of IL-2 produced were assayed by ELISA.

### *Immunoprecipitation and Western blot analysis*

A total of $5 \times 10^6$ 3DT52.5.8 T cell hybridoma CD4 transfectant cells was treated with medium alone or with IgG Ab (10 $\mu$g $ml^{-1}$) or with either the CD4-specific mAb OKT4 or L-68 (10 $\mu$g $ml^{-1}$); then immunoprecipitates were resolved by 12% SDS-PAGE and transferred onto nitrocellulose membranes (Amersham Biosciences). Blots were probed with either a rabbit anti-CD4 polyclonal Ab, a rabbit anti-$p56^{lck}$ polyclonal Ab, a rabbit anti-phospho-lck ($Tyr^{505}$) polyclonal Ab, or the mouse 4G10 anti-phosphotyrosine mAb, followed by peroxidase-conjugated secondary Ab. Blots were then developed using ECL (NEN Life Science Products) and autoradiography (Eastman Kodak).

### *Imaging*

A total of $7.5 \times 10^4$ A20 cells pulsed with SEB was mixed with $7.5 \times 10^4$ T cells loaded with 1 $\mu$M fura 2-AM or Rhodamine-X (Molecular Probes) in an 8-well glass-bottom chamber slide (Labtek/Nunc). For time-lapse experiments, images were taken every 30 s for 30 min. At each time point, we collected a differential interference contrast (DIC) image, either fura 2-AM or Rhodamine-X images and a 20-$\mu$m $z$-stack of fluorescent (CFP, YFP, FRET) images separated by either 1–3 $\mu$m for regular fluorescence imaging or 5–7 $\mu$m for FRET imaging. Fixed cell staining was done by briefly incubating $10^5$ 3DT52.5.8 T cell transfectants with $10^5$ A20 cells pulsed with 10 $\mu$g/ml SEB, at 37°C for 5 min. Fixed cell samples were Ab stained (PY20-PE) upon spotting cells on slides, then treated with antifade reagent (Bio-Rad), and the slides were sealed and imaged. Microscope control, data acquisition, and data analysis were performed in Metamorph (Universal Imaging). More detailed information is available in the supplemental material.[5]

### *Conjugate analysis*

For each type and condition, the frequency of conjugate formation and the percentage of $Ca^{2+}$ fluxing cells over a 30-min period were determined. For those cells that formed conjugates (stable for >2 min), we measured the duration of contact, the magnitude of $Ca^{2+}$ flux, and the magnitude of CD4 accumulation. More detailed information is available in the supplemental material.[5]

### *FRET analysis*

The energy transfer efficiency (E) was calculated as: $E = 1 - (F_{DA}/F_D)$, where $F_{DA}$ is the fluorescence intensity of donor (CFP) before acceptor (YFP) bleaching, while $F_D$ is the fluorescence intensity of donor (CFP) postbeaching (28, 30, 37). To determine real-time FRET signal, at each time and focal point we calculated (28, 38), the microFRET normalized to the donor concentration ($FRETN^C$) according to the formula: $FRETN^C$ = (Ff –Df(Fd/Dd) –Af(Fa/Aa))/Df. All data were analyzed using Metamorph (Universal Imaging). For all images analyzed, background was subtracted based on local fluorescence averaged from a user-specified, cell-free region of each image. An intensity mask on the YFP emission was used to limit the analysis to cell surface pixels. FRET images were derived in Metamorph using the $FRETN^C$ formula described above. No photobleaching correction was applied to images to preserve relative quantitative information. More detailed information is available in the supplemental material.[5]

[5] The online version of this article contains supplemental material.

## Results

### *Functional CD4 dimerization on the cell surface*

To investigate the role of CD4 dimerization in the formation of an IS via live FRET microscopy, CFP and YFP proteins were fused with the C terminus of human CD4 wild-type or human CD4 containing the K318E mutation. Although this mutation abrogates CD4 dimerization, it does not affect the conformational integrity of the CD4 molecule (23). The chimeric proteins were stably expressed in the $CD4^-CD8^-$ murine T cell hybridoma 3DT52.5.8 (17, 23, 31, 32).

To facilitate FRET and functional comparisons of wt and mutant transfectants, we selected clones with comparable CFP and YFP fluorescence, as well as for similar overall CD4 surface levels (Fig. 1, *A–C*) and demonstrated that they retain the ability to associate with $p56^{lck}$ (data not shown). To validate that the tagged versions of wt and mutant CD4 behave as previously observed, these cell lines were then challenged with CD4-dependent or -independent stimuli. The CD4 coreceptor enhances the IL-2 response triggered by presentation of superantigen SEB to the $V\beta8^+$ 3DT52.5.8 T cell hybridoma (17, 23). Superantigen stimulation has been shown previously to result in similar activation phenotype, including the kinetics and pattern of synapse formation, as compared with peptide Ag stimulation (39–43). As previously demonstrated, the K318E mutation diminishes the response to MHC class II-SEB complexes presented by two types of APCs (DAP (transfected fibroblast with human MHC class II molecules) and A20 (murine B cell)), but not to anti-CD3 stimulation (23) (Fig. 1, *D–F*). Similar results were also observed with several other independently derived transfectants (data not shown). Differences in IL-2 production from two types of APCs (DAP (transfected fibroblast with human MHC class II molecules) and A20 (murine B cell)) probably reside in the much greater MHC class II expression in the transfectant as well as in the xenotype of the MHC (44–47).

### *FRET analysis of CD4 dimers on resting and activated cells*

The previous data suggested a critical role for CD4 dimers in mediating T cell activation events. Using two independent methods of FRET analysis (data not shown), we have investigated the requirements and dynamics of CD4 dimers before and during IS formation upon antigenic recognition.

Both methods of FRET analysis demonstrated CD4 self-association on the resting cell surface as well as lower FRET levels of CD4 mutant (CD4mut) transfectants relative to their CD4wt counterparts (Figs. 2*A* and 3). Using the donor recovery method, the CD4wt displayed higher FRET efficiency (wt, noncoupled, total: $E = 7.3 \pm 0.3\%$) as compared with the CD4mut (mut, noncoupled, total: $E = 4.4 \pm 0.1\%$) (Fig. 2*A*).

To distinguish between FRET due to molecular crowding from FRET due to specific molecular interactions (48), we have analyzed the dependence of FRET on acceptor:donor ratios. Indeed, we show that in both wt and mutant transfectant cells, the degree of FRET, assessed by donor recovery upon acceptor photobleaching, is independent on the molecular ratio of acceptor to donor

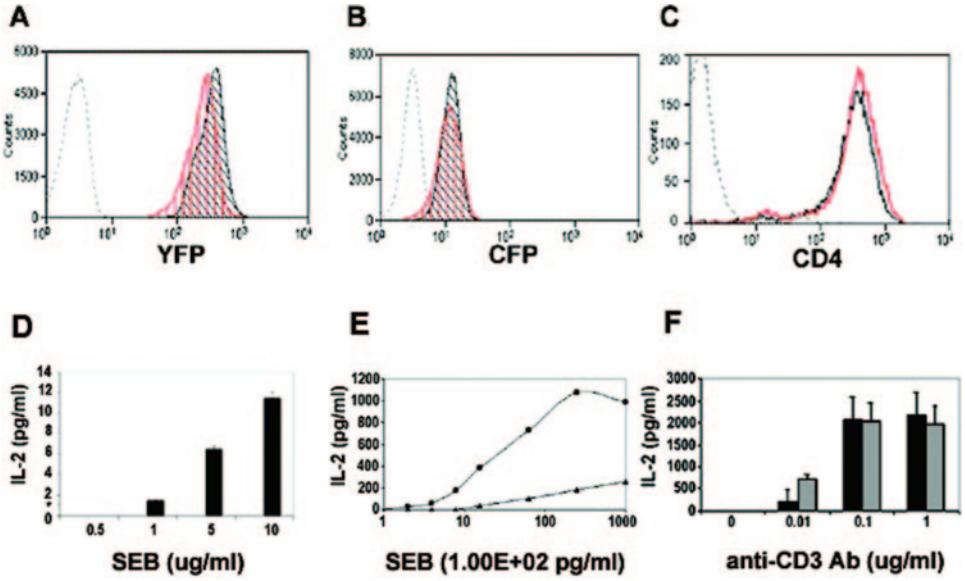


**FIGURE 1.** Equivalent surface expression, but altered function of CD4wt and CD4K318E CFP/YFP double transfectants. *A*, YFP fluorescence intensity; *B*, CFP fluorescence intensity; and *C*, cell surface CD4 levels of $CD4^-$ 3DT cells (gray dashed line), of 3DT CD4wt transfectants (solid black line), and of 3DT CD4mut transfectants (solid red line). The $CD4^-$ hybridomas transfected with CD4wt-CFP and CD4wt-YFP (CD4wt) (■) or with CD4mut-CFP and CD4mut-YFP (CD4mut) (▨) were stimulated with increasing concentrations of SEB presented by *D*, A20 cells; *E*, HLA-DR1-expressing DAP cells; or *F*, increasing doses of plate-coated anti-CD3 mAb (0.001 $\mu$g $ml^{-1}$; 0.1 $\mu$g $ml^{-1}$; 1 $\mu$g $ml^{-1}$), or left unstimulated (0 $\mu$g $ml^{-1}$ anti-CD3 Ab) as negative control. Supernatants were tested at 20 h for IL-2 by ELISA. *D*, The asterisk indicates the limit of detection of this assay. CD4mut IL-2 production was consistently below this limit.

(data not shown). This clearly demonstrates that the FRET signal observed in CD4 wt transfectants or in CD4 dimerization mutant transfectants is due to specific CD4 self-association, and does not result from the random distribution of CD4 proteins on the cellular membrane.

To further control for the observed FRET levels, we used calibration beads to determine that there are 82,324 and 106,434 CD4 molecules on the surface of wt and mutant transfectant cells, respectively, whereas published data reveal that there are ~98,000 CD4 molecules on the surface of Th cells of healthy human donors (49) (data not shown). This finding clearly demonstrates two important points: 1) the increased FRET signal observed on the surface of CD4wt transfectants as compared with CD4mut transfectants results from increased CD4 self-association, and is not due to higher surface density of CD4 molecules; 2) in our system, we assayed FRET at physiological levels, because the CD4 surface density on a molecule/cell basis of our wt and mutant transfectants is comparable to the CD4 surface density on normal human donors. Moreover, we demonstrate that CD4 dimers are present on the cellular membrane (data not shown). Altogether, these results provide clear proof that the only possible reason for increased FRET in the dimer-competent wt transfectant can only derive from the multimerization state (we suggest dimerization based on our previous biochemical studies).

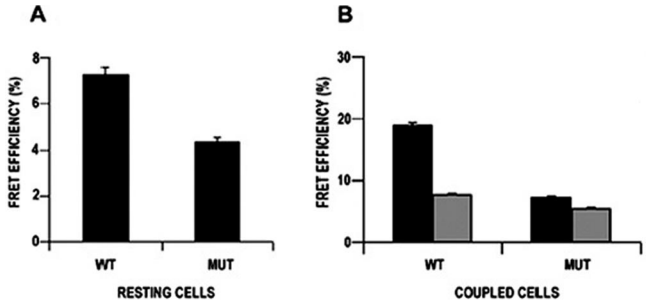


**FIGURE 2.** Quantitation of CD4 dimerization/oligomerization by FRET on T cell hybridomas. *A*, E was measured using a donor-recovery method (see *Materials and Methods* and supplemental material)[5] on the cell surface of CD4wt- or CD4mut-bearing T cell hybridomas resting (*A*) and coupled (*B*) during synapse formation for either the synapse region (average of all pixels in this region) (■), or for the nonsynapse (average of all pixels in this region) (▨). Data represent average and SDs for 85 cells.

We next investigated the requirements for and dynamics of CD4 dimers before and during immature IS formation upon antigenic recognition. The 3DT52.5.8 line, like other hybridomas (30), does not complete a mature c:central supramolecular activation cluster, but initiates immature synapse formation characterized by the accumulation of CD3, CD4, LFA-1, intracellular calcium release, and stable couples that typically last >20 min. Efficiency of energy transfer was quantified on fixed couples formed by the CD4 transfectants with the SEB-presenting A20 APCs (Fig. 2*B*). $FRETN^C$ was determined during coculture of the CD4 transfectants with the SEB-presenting A20 APCs (Fig. 3 and supplemental movies 1 and 2).[5] Both methods of FRET analysis (Figs. 2 and 3) clearly demonstrate that, on the outside or within the contact area at all time points, the CD4mut molecules displayed consistently lower compensated FRET levels than their CD4wt counterparts, reflecting the impairment of CD4K318E mutant molecules to dimerize (23). Interestingly, the CD4wt transfectant displayed highly increased FRET signal within the synapse area relative to the noncontact region: 19.0 ± 0.4% FRET efficiency at the contact area (wt, coupled, synapse) vs 7.8 ± 0.2% at the noncontact area (wt, coupled nonsynapse) (Fig. 2*B*). In contrast, the CD4mut transfectant displayed only marginally increased FRET signal at the contact area (mut, coupled, synapse: 7.2 ± 0.2%) relative to noncontact area (mut, coupled, nonsynapse: 5.4 ± 0.2%).

We did not observe any kinetic lapse between CD4 accumulation and increased FRET level (Fig. 3*A* and supplemental movie 1),[5] suggesting that synapse engagement of molecules is integral to the rise in FRET. Nonetheless, increased FRET at the IS might

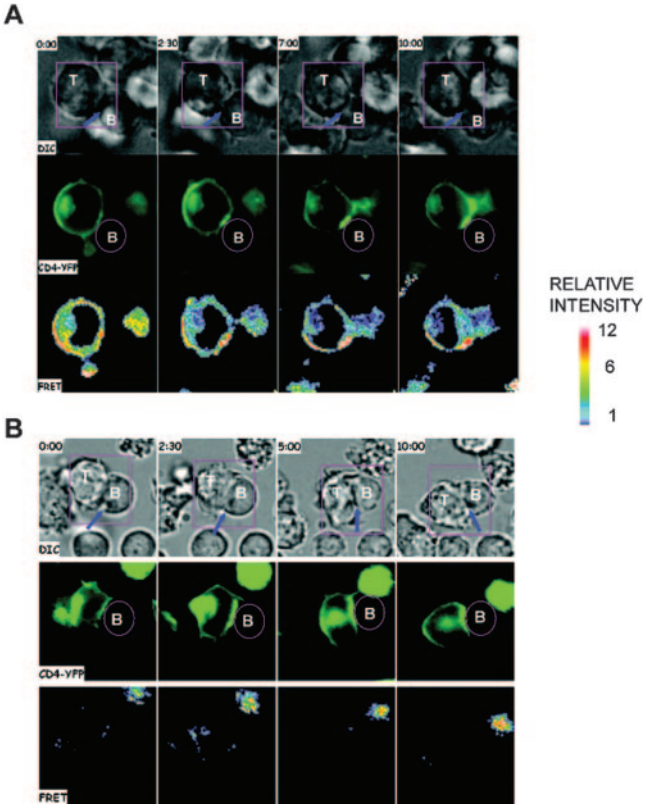


**FIGURE 3.** CD4 dimer, but not CD4 monomer displays increased FRET at the IS. CD4wt transfectants (*A*) or CD4mut transfectants (*B*) were imaged at 30-s intervals while interacting with SEB (10 $\mu$g ml$^{-1}$)-pulsed A20 B cells. Each time point shows the DIC image, a mid-cell z section of YFP, and the calculated FRET intensity. Times relative to the onset of cell-cell contact are indicated. This result has been confirmed in at least 10 couples for each condition. Fluorescence data for *A* and *B* are displayed on identical color scales (indicated).

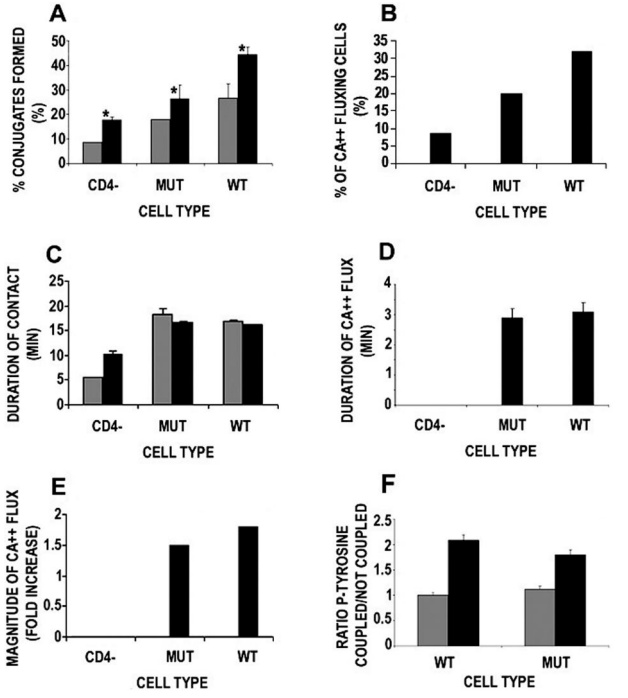


**FIGURE 4.** CD4 dimerization potentiates conjugate formation and signaling commitment, but has no effect on later stages of activation, including duration of contact, $Ca^{2+}$ flux, or total tyrosine phosphorylation. *A*, Percentage of conjugate formation, and *B*, percentage of $Ca^{2+}$ fluxing cells for CD4$^-$ cells, CD4wt, and CD4mut transfectants, in the presence (■) or in the absence (▨) of 10 $\mu$g ml$^{-1}$ SEB. The cells that formed stable conjugates (>2 min) were subsequently scored for *C*, duration of cell-cell contact; *D*, duration of $Ca^{2+}$ flux; and *E*, magnitude of $Ca^{2+}$ flux. Data shown were obtained from 72 (*n*, CD4$^-$), from 53 (*n*, MUT), and from 126 (*n*, WT) individual couples. *F*, Total tyrosine phosphorylation was measured in cells that formed stable conjugates (>2 min) in presence of Ag (■) or absence of Ag (▨). Data shown were obtained from 42 (*n*, WT) and from 44 (*n*, MUT) individual couples.

result from either multimeric clustering or from the formation of a tighter dimer of CD4wt molecules, and this cannot be distinguished at present.

### *CD4 dimers potentiate T cell-APC conjugate formation*

Having established that CD4 dimers are ubiquitously expressed on the cell surface and accumulate at the immature IS, we used the live-imaging approach to observe proximal events of cell-cell interaction, $Ca^{2+}$ flux, and synapse formation of T cell hybridomas bearing the chimeric molecules when incubated with APCs.

The CD4wt-expressing T cells formed stable conjugates more efficiently with Ag-pulsed A20 APCs than the CD4mut- or the CD4-negative-expressing T cells (44.3 vs 26.4 vs 17.7%) ($p < 0.005$). This trend was also observed in the absence of Ag (26.6 vs 18.0 vs 8.7%); however, it is not statistically significant (Fig. 4*A*). The novel finding in this study lies in that during antigenic stimulation CD4 dimer potentiates the T cell-APC adhesion as compared with CD4 monomer, implying that dimeric CD4 binds MHC class II with stronger avidity than its monomeric counterpart. It is noteworthy that we find a baseline conjugation level in our assay without either MHC class II or CD4, but that the presence of both these molecules dramatically augments this parameter (Fig. 4*A*, and data not shown).

### *CD4 dimers augment signaling commitment, but not duration*

In addition, CD4wt-expressing cells commit to signaling upon coupling with Ag-pulsed A20 APCs more efficiently than CD4mut- or CD4$^-$-expressing cells (percentage of $Ca^{2+}$ fluxing cells is 32 vs 20 vs 8.7%, respectively) (Fig. 4*B*). In CD4$^-$ cells, the $Ca^{2+}$ flux observed is either of low magnitude (≅1.2-fold increase over background) and/or of short duration (≅1 min). Therefore, these fluxing cells did not meet our scoring criteria and were not included in graphs in Fig. 4*D* (duration of $Ca^{2+}$ flux) and 4*E* (magnitude of $Ca^{2+}$ flux).

We further investigated the duration of contact in those cells that initiated stable conjugation (Fig. 4*C*, and data not shown) and showed that once couples are formed they have similar conjugate duration in cells expressing CD4wt or CD4mut, supporting a requirement for CD4 dimerization only in very early commitment.

In addition, the increase in $Ca^{2+}$ flux, either in terms of intensity or duration, was not appreciably different in cells bearing CD4wt or CD4mut molecules (CD4wt, peak intensity of $Ca^{2+}$ flux was 1.8-fold increase over background, and duration of $Ca^{2+}$ flux was 3.1 min; CD4mut, peak intensity of $Ca^{2+}$ flux was 1.5-fold increase over background, and duration of $Ca^{2+}$ flux was 2.9 min) (Figs. 4, *D* and *E*, and 5, and data not shown). In all cases, $Ca^{2+}$ flux was only observed upon specific TCR recognition irrespective of the APC type used, and was highly potentiated by CD4 as CD4$^-$ T cells display poor $Ca^{2+}$ flux upon stimulation (data not shown). Similar conjugate results were seen using other clones expressing these molecules under a variety of stimulation conditions, again demonstrating that the effects observed are due to CD4 dimerization state and not to clonal variation (data not shown).

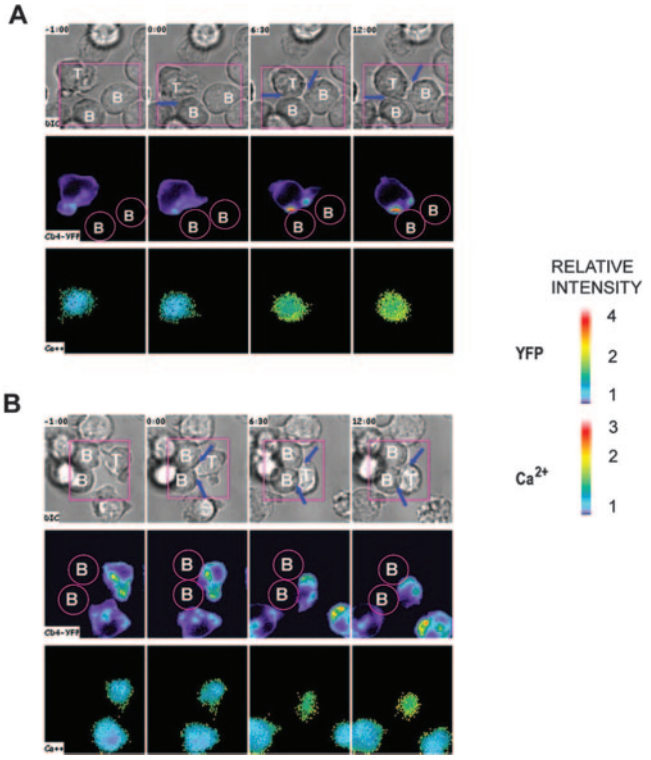


**FIGURE 5.** Examples of CD4 accumulation and $Ca^{2+}$ flux in CD4wt- and CD4mut-expressing cells. CD4wt (*A*) and CD4mut (*B*) transfectants were imaged at 30-s intervals while interacting with SEB (10 $\mu$g $ml^{-1}$)-pulsed A20 B cells. Each time point shows the DIC image, the $Ca^{2+}$ increase obtained with fura 2-AM, and a mid-cell *z* section of YFP. Times relative to the onset of cell-cell contact are indicated. Fluorescence data for *A* and *B* are displayed on identical color scales (indicated).

As another measure of activation status within already formed couples, we assessed the level of tyrosine phosphorylation in either wt or mutant transfectants upon coupling with APCs and have quantified the ratio of total tyrosine phosphorylation in coupled cells over not-coupled cells (Fig. 4*F*). Both CD4 wt- and CD4mut-expressing T cells displayed an increased level of total tyrosine phosphorylation when coupled with Ag-pulsed APCs, and there was no significant difference between CD4wt and CD4mut transfectants.

Whereas the CD4 dimeric form only is important for scanning and initial adhesion (that is CD4 dimers aid in initial stages of conjugate formation), the sum of this data indicates that either dimeric or monomeric forms are sufficient once a response has started.

### *Quantitatively augmented enrollment of CD4 dimers at the IS*

To gauge the level of CD4 recruitment to the synapse, we scored the distribution of CD4-YFP chimeric proteins in those cells that did form a stable conjugate. Within this population, the CD4 dimerization mutant was clearly defective in CD4 recruitment and persistence at the contact area (data not shown, Figs. 5 and 6). An example of persistent CD4wt accumulation at the synapse (≈2.8-fold increase lasting 9.2 min) is shown in Fig. 5*A*. In contrast, an example of inefficient accumulation of CD4mut molecules (1.8-fold increase, lasting 4.0 min) is shown in Fig. 5*B*. These differences, while only 2.8- vs 1.8-fold, are nevertheless statistically different and consistently reproduced in two independent systems (using either A20 or DAP cells as APCs). This result is consistent with a role for dimerization in increasing the affinity of CD4 for

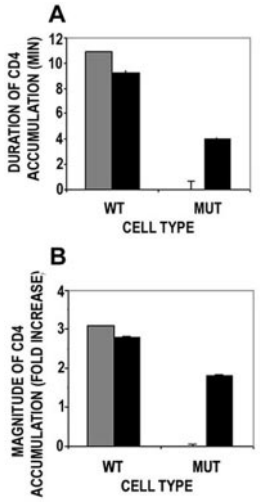


**FIGURE 6.** CD4mut are defective in Ag-independent and -dependent synapse accumulation. The cells that formed stable conjugates (>2 min) were scored for CD4 recruitment at the synapse in the presence (■) or absence (▨) of Ag. The duration (*A*) and magnitude (*B*) of CD4 recruitment were further scored in those cells that accumulated CD4. Data shown were obtained from 126 (*n*, WT) and from 53 (*n*, MUT) individual couples.

MHC and may explain larger dwell times in the presence or absence of Ag.

### *Differential phosphorylation of p56$^{lck}$* associated to either CD4wt or CD4mut molecules

Beyond effects on conjugate formation and CD4 accumulation, the $Ca^{2+}$ and phosphotyrosine data indicated that the dimer mutant is primarily defective in promoting signal initiation. This suggested that a triggering defect in the CD4 dimer mutant might be much more proximal, such as the ability of this molecule to successfully recruit lck. Although we have established that the dimer mutant successfully associates with lck (data not shown), this kinase is subjected to multiple levels of regulation. In particular, lck can be phosphorylated on $Tyr^{505}$, which results in autoinhibition, or can be phosphorylated on $Tyr^{394}$, which augments kinase function (50).

We assessed the phosphorylation state of lck in wild-type and mutant bearing cells, and we observed an increased $Tyr^{505}$ phosphorylation of lck associated to CD4mut as compared with lck associated to CD4wt, with no appreciable difference in total phosphotyrosine levels (Fig. 7*A*, and data not shown). Averaged over three independent experiments and normalized to total lck levels and loading in the immunoprecipitation, CD4mut had a ~1.95-fold increase in associated $Tyr^{505}$ (Fig. 7*B*), and mutant was always more highly associated with the $Tyr^{505}$ as compared with wt. Thus, the dimer mutation alters the balance of inhibited $lck^{505}$ loaded onto CD4.

## Discussion

In this study, we show evidence for the existence of CD4 dimers on T cells and multiple stage-specific requirements for their function. Specifically, these dimers are necessary for efficient initial CD4 accumulation, for TCR-dependent and -independent conjugate formation, and for the signaling onset leading to synapse development. Once an activation threshold is reached, CD4 dimer mutants display no defects beyond their accumulation within the IS.

### *FRET analysis of CD4 dimers*

A basal level of CD4 dimerization, observed in this study by FRET measurements, is consistent with previous biochemical studies

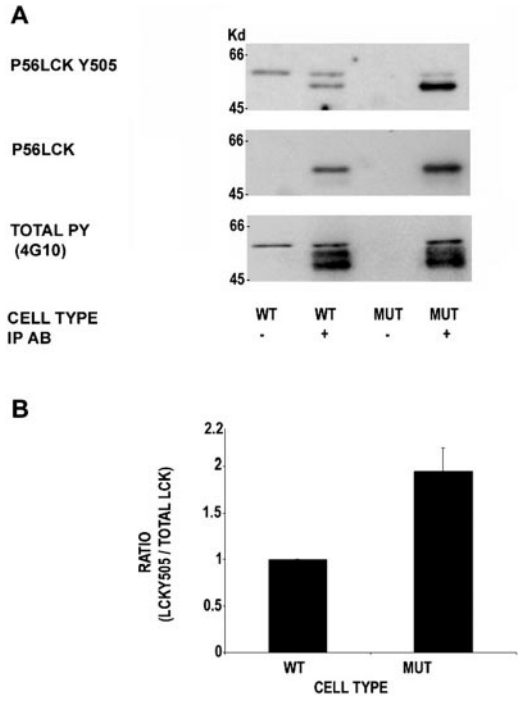


**FIGURE 7.** Differential phosphorylation of p56$^{lck}$ associated with either CD4wt or CD4mut molecules. *A*, Lysates from 3DT52.5.8 T cells expressing either CD4wt chimeric proteins or CD4mut chimeric proteins were immunoprecipitated with medium alone (*lanes 1* and *3*) or with the CD4-specific mAb OKT4 (*lanes 2* and *4*), then blotted with a phospho-*lck* (Tyr$^{505}$)-specific Ab, with a *lck*-specific Ab, and with a phospho-Tyr-specific Ab. The m.w. markers are indicated. *B*, The level of phosphorylated p56$^{lck}$ (Y505) was normalized to the level of total p56$^{lck}$ protein (total *lck*), and the ratio was graphed for both wt and mut transfectants. Data shown is the average ratio for three independent experiments.

showing CD4 dimers in resting cells (23, 51). Because overall density of cell surface CD4 molecules on the cell surface is comparable between wt and mut transfectants, the only possible reason for increased FRET (wt vs dimer mutant) is the dimerization or multimerization state.

Interestingly, the time-lapse FRET analysis shows that upon engagement at the synapse, CD4wt molecules exhibit an increase in the FRET ratio at the IS, concomitant with CD4 accumulation. At this time, there are four possible explanations for this observation: 1) close packing of dimers with one another; 2) alternative dimerization domains strengthening the pre-existing dimer; 3) conformational change in individual dimers upon ligand binding; and 4) dimerization of monomers at the synapse. It is interesting to note that a second minor CD4 self-association site, mapping to the FG and CC′ loops of the D1 extracellular domain, has been suggested by computer-modeling and functional studies (17, 22). Thereby, an appealing hypothesis is that CD4 dimerization is mediated via D4 domain, whereas CD4 oligomerization is potentiated by the D1 domain. Additional proteins, either intracellular or extracellular, might also promote CD4 dimerization/oligomerization. For example, before IS formation, the dimerization of the CD4-associated p56$^{lck}$ molecule might further strengthen CD4 oligomerization; at the IS, this would promote lck *trans*-phosphorylation, and ultimately enhance signaling (16). Also, during antigenic stimulation, CD4 oligomerization might be induced by binding to class II MHC molecules or to TCR molecules.

### *Stage-specific requirement for CD4 dimers*

We find that CD4 dimers are most important for the very early stages of IS formation. First, CD4 dimers facilitate conjugate formation in our system even in the absence of Ag, suggesting a role in facilitating adhesion and/or weak tonic signaling. This coincides with CD4 accumulation, providing a correlation between CD4 accumulation and adhesion. Second, in the presence of TCR agonist CD4 dimers promote stable long-lasting contacts that give rise to $Ca^{2+}$ signals. CD4mut expression is characterized by multiple transient contacts, which do not give rise to $Ca^{2+}$ signals and are most likely responsible for the decreased IL-2 levels in bulk assays. However, occasionally stable contacts are formed, and these result in similar $Ca^{2+}$ flux in CD4mut and CD4wt cells. Differential IL-2 secretion can also be explained by the fact that the threshold required to initiate $Ca^{2+}$ signaling is probably less stringent than cytokine secretion, as implied by the work of Valitutti et al. (52) and Hemmer et al. (53).

### *The role of CD4 dimerization in adhesion*

At the contact area, CD4 dimerization within the IS may increase the two-dimensional affinity of the interacting membranes and increase coupling duration. Indeed, the structure of the mature IS, composed of highly organized spatially segregated supramolecular activation clusters, provides a high local concentration of the interactive molecules and excludes nonbinding or inhibitory proteins such as CD45 or CD43 (24). Additionally, CD4 dimers may function at the contact area to localize and/or immobilize MHC class II molecules for TCR recognition. Irvine et al. (4) have suggested that for suboptimal receptor-ligand avidities, CD4 bridges a pseudodimer formed by agonist and null-peptide MHC and stabilizes weak TCR binding to the MHC-peptide complex. Based on crystallographic and mutagenesis data, Konig et al. (19) have previously speculated that oligomers of MHC class II molecules are stabilized by CD4 dimers. Finally, as indicated by solution studies, CD4 oligomerization may increase the avidity of the weak monomeric CD4-pMHC interaction (18).

Basal CD4 dimerization may be required for constitutive low-level tonic interaction with self pMHC complexes that may complement TCR partial engagement by self pMHC ligands in the peripheral immune system, supporting the stochastic resonance concept proposed by Germain and Stefanova (54). Interestingly, work by Bottomly and coworkers (55) elegantly demonstrates that CD4 ligation inhibits memory, but not naive T cells. This supports the hypothesis that CD4 dimerization status may modulate T cell activation threshold, allowing for tonic interaction of naive T cells with self MHC molecules, but preventing irrelevant and potentially dangerous interactions between memory T cells and bystander MHC class II$^+$ cells.

### *CD4 dimers are associated with preactivated p56$^{lck}$*

Recent studies suggest that CD4 boosts activation and synapse formation by enhancing TCR signaling (10). Our data support the hypothesis that CD4 dimers are important for the recruitment of a preactivated form of lck to the synapse because the CD4mut with increased Tyr$^{505}$ phosphorylation levels on its associated lck is defective at initiating $Ca^{2+}$ signaling. Dimer clustering at the synapse may also provide the associated preactivated p56$^{lck}$ with a high local concentration of signaling and adaptor molecules, favorable for both lck transphorylation and activity of downstream players. In support for a role of CD4 in TCR triggering, it has been demonstrated that optimal antigenic stimulation involves intermolecular interaction between CD4 and TCR molecules at the synapse (30). In this way, lck may be allowed to phosphorylate the

TCR-associated, signal-transducing CD3 polypeptides (30, 56, 57). A 2-fold difference in the phosphorylation state of the critical proximal kinase for TCR stimulation may well have much larger downstream effects, thus explaining the decreased IL-2 production by the mutant, to a level even below $CD4^-$ cells (23).

It can thus be inferred that the balance between monomeric and dimeric forms of CD4 modulates the threshold of T cell activation. In this aspect, it would be interesting to quantify and compare the proportion of dimeric CD4 molecules on the surface of thymocytes vs peripheral lymphocytes, naive vs memory T lymphocytes, or primed vs anergic T cells. Furthermore, viral escape mechanisms may include biasing the proportion of CD4 dimers in favor of monomers on the cell surface. Whether CD4 dimerization is regulated from the inside (e.g., lck dissociation, binding of intracellular ligands (linker for activation of T cells, ACP33) or viral proteins (HIV nef), raft localization) or from the outside (e.g., extracellular membrane-bound or soluble ligands (e.g., IL-16, HIV gp120/160), redox potential of extracellular matrix) remains to be investigated.

## Acknowledgments

We thank C. Estrela for secretarial assistance; C. McArthur for assistance with FRET measurements on FACS; and A. Weiss, M. Davis, and N. Killeen for critical reading of the manuscript.

## Disclosures

The authors have no financial conflict of interest.

## References

1. Marrack, P., R. Endres, R. Shimonkevitz, A. Zlotnik, D. Dialynas, F. Fitch, and J. Kappler. 1983. The major histocompatibility complex-restricted antigen receptor on T cells. II. Role of the L3T4 product. *J. Exp. Med.* 158: 1077–1091.
2. Hampl, J., Y. H. Chien, and M. M. Davis. 1997. CD4 augments the response of a T cell to agonist but not to antagonist ligands. *Immunity* 7: 379–385.
3. Madrenas, J., L. A. Chau, J. Smith, J. A. Bluestone, and R. N. Germain. 1997. The efficiency of CD4 recruitment to ligand-engaged TCR controls the agonist/partial agonist properties of peptide-MHC molecule ligands. *J. Exp. Med.* 185: 219–229.
4. Irvine, D. J., M. A. Purbhoo, M. Krogsgaard, and M. M. Davis. 2002. Direct observation of ligand recognition by T cells. *Nature* 419: 845–849.
5. Vidal, K., B. L. Hsu, C. B. Williams, and P. M. Allen. 1996. Endogenous altered peptide ligands can affect peripheral T cell responses. *J. Exp. Med.* 183: 1311–1321.
6. Leitenberg, D., Y. Boutin, S. Constant, and K. Bottomly. 1998. CD4 regulation of TCR signaling and T cell differentiation following stimulation with peptides of different affinities for the TCR. *J. Immunol.* 161: 1194–1203.
7. Konig, R., S. Fleury, and R. N. Germain. 1996. The structural basis of CD4-MHC class II interactions: coreceptor contributions to T cell receptor antigen recognition and oligomerization-dependent signal transduction. *Curr. Top. Microbiol. Immunol.* 205: 19–46.
8. Veillette, A., M. A. Bookman, E. M. Horak, and J. B. Bolen. 1988. The CD4 and CD8 T cell surface antigens are associated with the internal membrane tyrosine-protein kinase $p56^{lck}$. *Cell* 55: 301–308.
9. Veillette, A., M. A. Bookman, E. M. Horak, L. E. Samelson, and J. B. Bolen. 1989. Signal transduction through the CD4 receptor involves the activation of the internal membrane tyrosine-protein kinase $p56^{lck}$. *Nature* 338: 257–259.
10. Holdorf, A. D., K. H. Lee, W. R. Burack, P. M. Allen, and A. S. Shaw. 2002. Regulation of Lck activity by CD4 and CD28 in the immunological synapse. *Nat. Immunol.* 3: 259–264.
11. Doyle, C., and J. L. Strominger. 1987. Interaction between CD4 and class II MHC molecules mediates cell adhesion. *Nature* 330: 256–259.
12. Cammarota, G., A. Scheirle, B. Takacs, D. M. Doran, R. Knorr, W. Bannwarth, J. Guardiola, and F. Sinigaglia. 1992. Identification of a CD4 binding site on the $\beta 2$ domain of HLA-DR molecules. *Nature* 356: 799–801.
13. Konig, R., L. Y. Huang, and R. N. Germain. 1992. MHC class II interaction with CD4 mediated by a region analogous to the MHC class I binding site for CD8. *Nature* 356: 796–798.
14. Brogdon, J., D. D. Eckels, C. Davies, S. White, and C. Doyle. 1998. A site for CD4 binding in the $\beta 1$ domain of the MHC class II protein HLA-DR1. *J. Immunol.* 161: 5472–5480.
15. Xiong, Y., P. Kern, H. Chang, and E. Reinherz. 2001. T cell receptor binding to a pMHCII ligand is kinetically distinct from and independent of CD4. *J. Biol. Chem.* 276: 5659–5667.
16. Wu, H., P. D. Kwong, and W. A. Hendrickson. 1997. Dimeric association and segmental variability in the structure of human CD4. *Nature* 387: 527–530.
17. Huang, B., A. Yachou, S. Fleury, W. A. Hendrickson, and R. P. Sekaly. 1997. Analysis of the contact sites on the CD4 molecule with class II MHC molecule: co-ligand versus co-receptor function. *J. Immunol.* 158: 216–225.
18. Weber, S., and K. Karjalainen. 1993. Mouse CD4 binds MHC class II with extremely low affinity. *Int. Immunol.* 5: 695–698.
19. Konig, R., X. Shen, and R. N. Germain. 1995. Involvement of both major histocompatibility complex class II $\alpha$ and $\beta$ chains in CD4 function indicates a role for ordered oligomerization in T cell activation. *J. Exp. Med.* 182: 779–787.
20. Sakihama, T., A. Smolyar, and E. L. Reinherz. 1995. Oligomerization of CD4 is required for stable binding to class II major histocompatibility complex proteins but not for interaction with human immunodeficiency virus gp120. *Proc. Natl. Acad. Sci. USA* 92: 6444–6448.
21. Satoh, T., S. Li, T. M. Friedman, R. Wiaderkiewicz, R. Korngold, and Z. Huang. 1996. Synthetic peptides derived from the fourth domain of CD4 antagonize off function and inhibit T cell activation. *Biochem. Biophys. Res. Commun.* 224: 438–443.
22. Li, S., J. Gao, T. Satoh, T. M. Friedman, A. E. Edling, U. Koch, S. Choksi, X. Han, R. Korngold, and Z. Huang. 1997. A computer screening approach to immunoglobulin superfamily structures and interactions: discovery of small non-peptidic CD4 inhibitors as novel immunotherapeutics. *Proc. Natl. Acad. Sci. USA* 94: 73–78.
23. Moldovan, M. C., A. Yachou, K. Levesque, H. Wu, W. A. Hendrickson, E. A. Cohen, and R. P. Sekaly. 2002. CD4 dimers constitute the functional component required for T cell activation. *J. Immunol.* 169: 6261–6268.
24. Monks, C. R., B. A. Freiberg, H. Kupfer, N. Sciaky, and A. Kupfer. 1998. Three-dimensional segregation of supramolecular activation clusters in T cells. *Nature* 395: 82–86.
25. Grakoui, A., S. K. Bromley, C. Sumen, M. M. Davis, A. S. Shaw, P. M. Allen, and M. L. Dustin. 1999. The immunological synapse: a molecular machine controlling T cell activation. *Science* 285: 221–227.
26. Krummel, M. F., M. D. Sjaastad, C. Wulfing, and M. M. Davis. 2000. Differential clustering of CD4 and CD3$\zeta$ during T cell recognition. *Science* 289: 1349–1352.
27. Ehrlich, L. I., P. J. Ebert, M. F. Krummel, A. Weiss, and M. M. Davis. 2002. Dynamics of $p56^{lck}$ translocation to the T cell immunological synapse following agonist and antagonist stimulation. *Immunity* 17: 809–822.
28. Gordon, G. W., G. Berry, X. H. Liang, B. Levine, and B. Herman. 1998. Quantitative fluorescence resonance energy transfer measurements using fluorescence microscopy. *Biophys. J.* 74: 2702–2713.
29. Lippincott-Schwartz, J., E. Snapp, and A. Kenworthy. 2001. Studying protein dynamics in living cells. *Nat. Rev. Mol. Cell Biol.* 2: 444–456.
30. Zal, T., M. A. Zal, and N. R. Gascoigne. 2002. Inhibition of T cell receptor-coreceptor interactions by antagonist ligands visualized by live FRET imaging of the T-hybridoma immunological synapse. *Immunity* 16: 521–534.
31. Gay, D., P. Maddon, R. Sekaly, M. A. Talle, M. Godfrey, E. Long, G. Goldstein, L. Chess, R. Axel, and J. Kappler. 1987. Functional interaction between human T-cell protein CD4 and the major histocompatibility complex HLA-DR antigen. *Nature* 328: 626–629.
32. Greenstein, J. L., J. Kappler, P. Marrack, and S. J. Burakoff. 1984. The role of L3T4 in recognition of Ia by a cytotoxic, $H\text{-}2D^d$-specific T cell hybridoma. *J. Exp. Med.* 159: 1213–1224.
33. Pear, W. S., G. P. Nolan, M. L. Scott, and D. Baltimore. 1993. Production of high-titer helper-free retroviruses by transient transfection. *Proc. Natl. Acad. Sci. USA* 90: 8392–8396.
34. Kim, K. J., C. Kanellopoulos-Langevin, R. M. Merwin, D. H. Sachs, and R. Asofsky. 1979. Establishment and characterization of BALB/c lymphoma lines with B cell properties. *J. Immunol.* 122: 549–554.
35. Fleury, S., D. Lamarre, S. Meloche, S. E. Ryu, C. Cantin, W. A. Hendrickson, and R. P. Sekaly. 1991. Mutational analysis of the interaction between CD4 and class II MHC: class II antigens contact CD4 on a surface opposite the gp120-binding site. *Cell* 66: 1037–1049.
36. Leo, O., M. Foo, D. H. Sachs, L. E. Samelson, and J. A. Bluestone. 1987. Identification of a monoclonal antibody specific for a murine T3 polypeptide. *Proc. Natl. Acad. Sci. USA* 84: 1374–1378.
37. Kenworthy, A. K. 2001. Imaging protein-protein interactions using fluorescence resonance energy transfer microscopy. *Methods* 24: 289–296.
38. Sorkin, A., M. McClure, F. Huang, and R. Carter. 2000. Interaction of EGF receptor and *grb2* in living cells visualized by fluorescence resonance energy transfer (FRET) microscopy. *Curr. Biol.* 10: 1395–1398.
39. Glaichenhaus, N., N. Shastri, D. R. Littman, and J. M. Turner. 1991. Requirement for association of $p56^{lck}$ with CD4 in antigen-specific signal transduction in T cells. *Cell* 64: 511–520.
40. Morgan, M. M., C. M. Labno, G. A. van Seventer, M. F. Denny, D. B. Straus, and J. K. Burkhardt. 2001. Superantigen-induced T cell:B cell conjugation is mediated by LFA-1 and requires signaling through Lck, but not Zap-70. *J. Immunol.* 167: 5708–5718.
41. Sancho, D., M. C. Montoya, A. Monjas, M. Gordon-Alonso, T. Katagiri, D. Gil, R. Tejedor, B. Alarcon, and F. Sanchez-Madrid. 2002. TCR engagement induces proline-rich tyrosine kinase-2 (Pyk2) translocation to the T cell-APC interface independently of Pyk2 activity and in an immunoreceptor tyrosine-based activation motif-mediated fashion. *J. Immunol.* 169: 292–300.
42. Pizzo, P., E. Giurisato, A. Bigsten, M. Tassi, R. Tavano, A. Shaw, and A. Viola. 2004. Physiological T cell activation starts and propagates in lipid rafts. *Immunol. Lett.* 91: 3–9.
43. Wulfing, C., A. Bauch, G. R. Crabtree, and M. M. Davis. 2000. The *vav* exchange factor is an essential regulator in actin-dependent receptor translocation to the lymphocyte-antigen-presenting cell interface. *Proc. Natl. Acad. Sci. USA* 97: 10150–10155.
44. Stohl, W., J. E. Elliott, and P. S. Linsley. 1994. Polyclonal in vitro T cell proliferation and T cell-dependent B cell differentiation supported by activated autologous B cells. *Clin. Immunol. Immunopathol.* 72: 44–52.

45. Stohl, W., D. Xu, S. Zang, K. S. Kim, L. Li, J. A. Hanson, S. A. Stohlman, C. S. David, and C. O. Jacob. 2001. In vivo staphylococcal superantigen-driven polyclonal Ig responses in mice: dependence upon $CD4^+$ cells and human MHC class II. *Int. Immunol.* 13: 1291–1300.
46. Cole, B. C., A. D. Sawitzke, E. A. Ahmed, C. L. Atkin, and C. S. David. 1997. Allelic polymorphisms at the H-2A and HLA-DQ loci influence the response of murine lymphocytes to the *Mycoplasma arthritidis* superantigen MAM. *Infect. Immun.* 65: 4190–4198.
47. Proft, T., S. L. Moffatt, C. J. Berkahn, and J. D. Fraser. 1999. Identification and characterization of novel superantigens from *Streptococcus pyogenes*. *J. Exp. Med.* 189: 89–102.
48. Kenworthy, A. K., and M. Edidin. 1998. Distribution of a glycosylphosphatidylinositol-anchored protein at the apical surface of MDCK cells examined at a resolution of <100 A using imaging fluorescence resonance energy transfer. *J. Cell Biol.* 142: 69–84.
49. Davis, K. A., B. Abrams, S. B. Iyer, R. A. Hoffman, and J. E. Bishop. 1998. Determination of CD4 antigen density on cells: role of antibody valency, avidity, clones, and conjugation. *Cytometry* 33: 197–205.
50. Weil, R., and A. Veillette. 1996. Signal transduction by the lymphocyte-specific tyrosine protein kinase $p56^{lck}$. *Curr. Top. Microbiol. Immunol.* 205: 63–87.
51. Lynch, G. W., A. J. Sloane, V. Raso, A. Lai, and A. L. Cunningham. 1999. Direct evidence for native CD4 oligomers in lymphoid and monocytoid cells. *Eur. J. Immunol.* 29: 2590–2602.
52. Valitutti, S., S. Muller, M. Dessing, and A. Lanzavecchia. 1996. Different responses are elicited in cytotoxic T lymphocytes by different levels of T cell receptor occupancy. *J. Exp. Med.* 183: 1917–1921.
53. Hemmer, B., I. Stefanova, M. Vergelli, R. N. Germain, and R. Martin. 1998. Relationships among TCR ligand potency, thresholds for effector function elicitation, and the quality of early signaling events in human T cells. *J. Immunol.* 160: 5807–5814.
54. Germain, R. N., and I. Stefanova. 1999. The dynamics of T cell receptor signaling: complex orchestration and the key roles of tempo and cooperation. *Annu. Rev. Immunol.* 17: 467–522.
55. Farber, D. L., M. Luqman, O. Acuto, and K. Bottomly. 1995. Control of memory CD4 T cell activation: MHC class II molecules on APCs and CD4 ligation inhibit memory but not naive CD4 T cells. *Immunity* 2: 249–259.
56. Rojo, J. M., K. Saizawa, and C. A. Janeway, Jr. 1989. Physical association of CD4 and the T-cell receptor can be induced by anti-T-cell receptor antibodies. *Proc. Natl. Acad. Sci. USA* 86: 3311–3315.
57. Vignali, D. A., R. T. Carson, B. Chang, R. S. Mittler, and J. L. Strominger. 1996. The two membrane proximal domains of CD4 interact with the T cell receptor. *J. Exp. Med.* 183: 2097–2107.